Studying nucleon structure via Double Deeply Virtual Compton Scattering (DDVCS)

Shengying ZHAO

10 Sep 2018

Institut de Physique Nucléaire Orsay, IN2P3/CNRS
ED PHENIICS, Université Paris-Sud & Paris-Saclay

Nucleon structure

Elastic electron scattering

$$e + p \to e + p$$

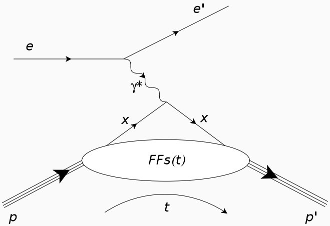

R. Hofstadter, Nobel Prize 1961

established the extended nature of the nucleon.

Form Factors (FFs) $\to$ nucleon size.

Deeply Inelastic Scattering (DIS)

$$e + p \to e + X$$

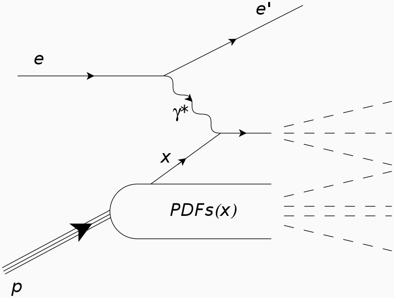

Friedman, Kendall, Taylor, Nobel Prize 1990

discovered the existence of quarks inside the nucleon.

Parton Distribution Functions (PDFs) $\to$ parton longitudinal momentum.

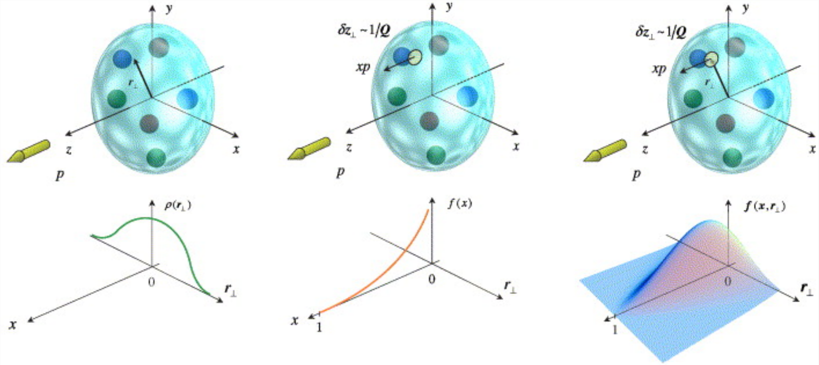

Form Factors
transverse profile

Parton Distribution Functions
longitudinal momentum distribution

Generalized Parton Distributions (GPDs) nucleon tomography from the correlation between transverse position and longitudinal momentum of partons

Nucleon structure - Generalized Parton Distributions (GPDs)

GPDs are 4 universal functions, $H^q, E^q, \widetilde{H}^q, \widetilde{E}^q(x, \xi, t)$ $(H^g, E^g, \widetilde{H}^g, \widetilde{E}^g)$, describing the non-perturbative quark (gluon) structure of the nucleon [1-3]. They correspond to the probability of picking a quark with a longitudinal momentum fraction $x + \xi$ and inserting it back with $x - \xi$.

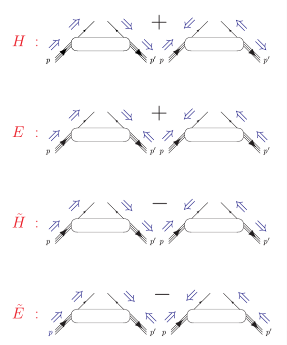

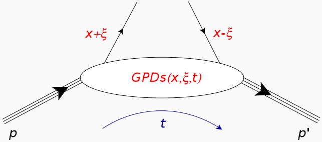

- x - the initial longitudinal momentum fraction of partons;
- ξ - the transferred longitudinal momentum fraction or skewness parameter;
- t - the square of momentum transfer to the nucleon.

[1] D. Müller, *et al.*, Fortschr. Phys. **42**, 101 (1994). [2] A.V. Radyushkin, Phys. Rev. D **56**, 5524 (1997).
[3] X. Ji, Phys. Rev. Lett. **78**, 610 (1997).

Nucleon structure - GPDs Measurements

DVCS and DDVCS [4-6] are two golden processes for direct measurements of GPDs

$ep \to ep\gamma$

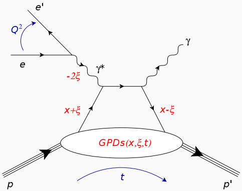

Deeply Virtual Compton Scattering (DVCS)

$ep \to epl^- l^+$

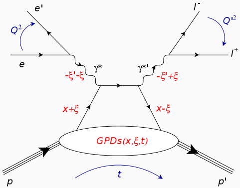

Double DVCS (DDVCS)

$$\mathcal{H}(\xi,\xi,t) = \sum_q e_q^2 \Big\{ \mathcal{P}\int_{-1}^{1} dx\, H^q(x,\xi,t)\left[\frac{1}{x-\xi}+\frac{1}{x+\xi}\right] - i\pi\left[H^q(\xi,\xi,t)-H^q(-\xi,\xi,t)\right]\Big\}$$

$$\mathcal{H}(\xi',\xi,t) = \sum_q e_q^2 \Big\{ \mathcal{P}\int_{-1}^{1} dx\, H^q(x,\xi,t)\left[\frac{1}{x-\xi'}+\frac{1}{x+\xi'}\right] - i\pi\left[H^q(\xi',\xi,t)-H^q(-\xi',\xi,t)\right]\Big\}$$

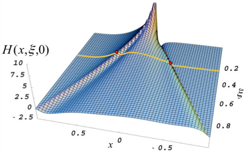

- DVCS can access GPDs only at $x = \pm\xi$;
- DDVCS allows one to measure the GPDs for each x, ξ, t values independently ($|\xi'| < \xi$).

[4] M. Guidal and M. Vanderhaeghen, Phys. Rev. Lett. **90** 012001 (2003).
[5] A. V. Belitsky and D. Müller, Phys. Rev. Lett. **90** 022001 (2003).
[6] I. V. Anikin, *et al.*, arXiv:1712.04198 (2017).

Feasibilitical study of DDVCS ($ep \to e'p'\mu^-\mu^+$) experiment at **JLab 12GeV**.

- Kinematics & phase space
- Projections of experimental observables & precision

The interpretation of the process is the most straightforward when the final leptons are muons, which avoids complex antisymmetrization issues.

Phase space & binning

Kinematic cuts:

- $W > 2$ GeV to ensure the deep inelastic scattering regime;
- $Q^2 > 1\ (\mathrm{GeV}/c^2)^2$ to ensure the reaction at parton level;
- $t > -1\ (\mathrm{GeV}/c^2)^2$ to support the factorization regime;
- $Q'^2 > (2m_\mu)^2$ to ensure the production of a di-muon pair.

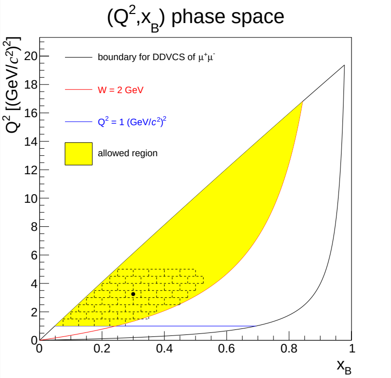

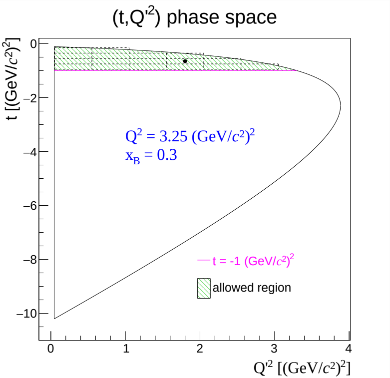

ΔQ^2 $(\mathrm{GeV}/c^2)^2$	Δx_B	$\Delta(-t)$ $(\mathrm{GeV}/c^2)^2$	$\Delta Q'^2$ $(\mathrm{GeV}/c^2)^2$	$\Delta\phi$ (degree)
0.5	0.05	0.2	0.5	15

664 four-dimensional(Q^2, x_B, t and Q'^2) bins have been firstly studied, each has 24 bins in ϕ.

Experimental observables - 7-fold differential cross section

$$\frac{d^7\sigma}{dQ^2 dx_{\mathrm{B}} d(-t) dQ'^2 d\phi d\theta_\mu d\varphi_\mu} \propto |\mathcal{T}_{\mathrm{BH}_1} + \mathcal{T}_{\mathrm{BH}_2} + \mathcal{T}_{\mathrm{VCS}}|^2$$

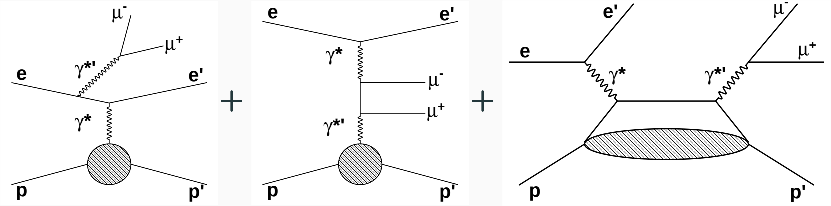

$$\begin{aligned}\sigma^e_{P0} \quad = \quad & \sigma_{\mathrm{BH1}} + \sigma_{\mathrm{BH2}} + (-e)\sigma_{\mathrm{BH12}} \\ & +\sigma_{\mathrm{VCS}} + P\widetilde{\sigma}_{\mathrm{VCS}} \\ & +(-e)(\sigma_{\mathrm{INT1}} + P\widetilde{\sigma}_{\mathrm{INT1}}) + \sigma_{\mathrm{INT2}} + P\widetilde{\sigma}_{\mathrm{INT2}}\end{aligned}$$

σ is sensitive to the real part of CFF and $\widetilde{\sigma}$ to the imaginary part.

Currently, there is no stable polarized target working under extremely high luminosity.

Experimental observables - 5-fold differential cross section

$$\frac{d^7\sigma}{dQ^2 dx_{\mathrm{B}} d(-t) dQ'^2 d\phi d\theta_\mu d\varphi_\mu} \propto |\mathcal{T}_{\mathrm{BH}_1} + \mathcal{T}_{\mathrm{BH}_2} + \mathcal{T}_{\mathrm{VCS}}|^2$$

$$\to \frac{d^5\sigma}{dQ^2 dx_{\mathrm{B}} d(-t) dQ'^2 d\phi} \propto |\mathcal{T}_{\mathrm{BH}_1} + \mathcal{T}_{\mathrm{VCS}}|^2 + |\mathcal{T}_{\mathrm{BH}_2}|^2,$$ to increase the statistics.

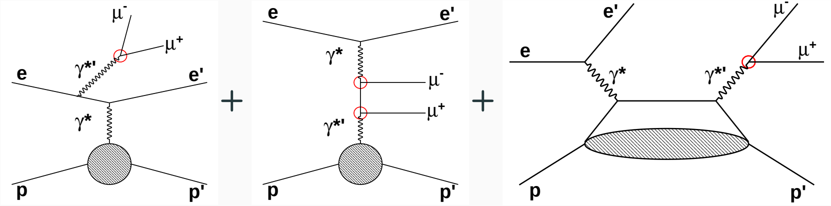

$\mathcal{T}_{\mathrm{BH}_1} \propto e_\mu$ $\mathcal{T}_{\mathrm{BH}_2} \propto e_\mu^2$ $\mathcal{T}_{\mathrm{VCS}} \propto e_\mu$

in center of mass frame

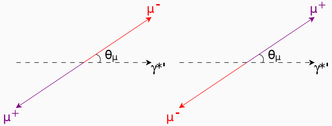

$\theta_\mu \to \pi - \theta_\mu,\ \varphi_\mu \to \pi + \varphi_\mu$

$$\begin{aligned} \sigma^e_{P0} \quad = \quad & \sigma_{\mathrm{BH1}} + \sigma_{\mathrm{BH2}} + \cancel{(-e)\sigma_{\mathrm{BH12}}} \\ & + \sigma_{\mathrm{VCS}} + P\widetilde{\sigma}_{\mathrm{VCS}} \\ & + (-e)(\sigma_{\mathrm{INT1}} + P\widetilde{\sigma}_{\mathrm{INT1}}) + \cancel{\sigma_{\mathrm{INT2}}} + \cancel{P\widetilde{\sigma}_{\mathrm{INT2}}} \end{aligned}$$

Experimental observables

$$\frac{d^7\sigma}{dQ^2 dx_{\mathrm{B}} d(-t) dQ'^2 d\phi d\theta_\mu d\varphi_\mu} \propto |\mathcal{T}_{\mathrm{BH}_1} + \mathcal{T}_{\mathrm{BH}_2} + \mathcal{T}_{\mathrm{VCS}}|^2$$
$$\frac{d^5\sigma}{dQ^2 dx_{\mathrm{B}} d(-t) dQ'^2 d\phi} \propto |\mathcal{T}_{\mathrm{BH}_1} + \mathcal{T}_{\mathrm{VCS}}|^2 + |\mathcal{T}_{\mathrm{BH}_2}|^2$$

$$\begin{aligned}\sigma^e_{P0} \quad = \quad & \sigma_{\mathrm{BH1}} + \sigma_{\mathrm{BH2}} + \cancel{(-e)\sigma_{\mathrm{BH12}}} \\ & + \sigma_{\mathrm{VCS}} + P\widetilde{\sigma}_{\mathrm{VCS}} \\ & + (-e)(\sigma_{\mathrm{INT1}} + P\widetilde{\sigma}_{\mathrm{INT1}}) + \cancel{\sigma_{\mathrm{INT2}}} + \cancel{P\widetilde{\sigma}_{\mathrm{INT2}}}\end{aligned}$$

- BH terms are calculable since the nucleon form factors are well known at small t;
- VCS terms are related to bilinear combinations of the CFFs;
- INT terms are related to linear combinations of the CFFs and the nucleon form factors.

$$\begin{cases} \sigma_{\mathrm{UU}} = \frac{1}{2}\left(\sigma^-_{+0} + \sigma^-_{-0}\right) & = \sigma_{\mathrm{BH1}} + \sigma_{\mathrm{BH2}} + \sigma_{\mathrm{VCS}} + \sigma_{\mathrm{INT1}} \\ \Delta\sigma_{\mathrm{LU}} = \frac{1}{2}\left(\sigma^-_{+0} - \sigma^-_{-0}\right) & = \widetilde{\sigma}_{\mathrm{VCS}} + \widetilde{\sigma}_{\mathrm{INT1}} \\ \Delta\sigma^{\mathrm{C}} = \frac{1}{2}\left(\sigma^-_{00} - \sigma^+_{00}\right) & = \sigma_{\mathrm{INT1}} \quad \text{(need positron beam)} \end{cases}$$

Measurement of $\frac{d^5\sigma}{dQ^2 dx_{\mathrm{B}} d(-t) dQ'^2 d\phi}$ as a function of ϕ needs a muon detector of 4π acceptance

Projections

The following conditions or assumptions have been applied:

- Luminosity: $\mathscr{L} = 10^{37}\ \mathrm{cm}^{-2}\mathrm{s}^{-1}$; Running time: 100 days;
- Detectors of 4π acceptance for the electrons/positrons and the di-muon pairs; Efficiency: 100%.

The number of events, for each five-dimensional bins (Q^2, x_B, t, Q'^2 and ϕ), has been computed as:

$$N = \frac{d\sigma}{dQ^2 dx_\mathrm{B} d(-t) dQ'^2 d\phi} \cdot \Delta Q^2 \cdot \Delta x_\mathrm{B} \cdot \Delta t \cdot \Delta Q'^2 \cdot \Delta\phi \cdot \mathscr{L} \cdot T$$

where $\frac{d\sigma}{dQ^2 dx_\mathrm{B} d(-t) dQ'^2 d\phi}$ is the 5-fold differential cross section computed by VGG model [7] based on the center value of each bin.

	total bin	$\delta\sigma_{\mathrm{UU}}/\sigma_{\mathrm{UU}}$ <10%	$\delta\Delta\sigma_{\mathrm{LU}}/\Delta\sigma_{\mathrm{LU}}$ <10%	$\delta\Delta\sigma^{\mathrm{C}}/\Delta\sigma^{\mathrm{C}}$ <10%
number of bins	664	544	46	148
ratio		82%	7%	22%

[7] I. V. M. Vanderhaeghen, P. A. M. Guichon and M. Guidal, Phys. Rev D, **60**, 094017 (1999).

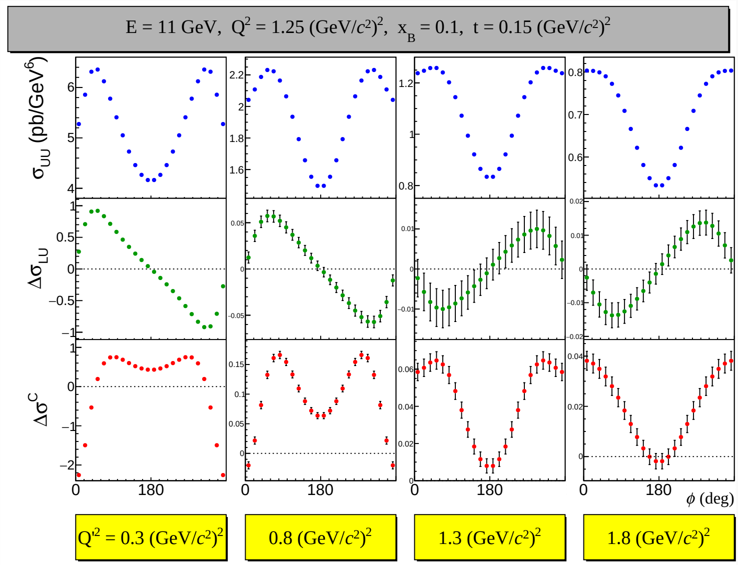

Q'^2 dependence:

- The cross sections and precisions decrease with increased Q'^2 ($Q'^2 = 0$ is equivalent to the DVCS process having the largest cross section);
- $\Delta\sigma_{\mathrm{LU}}$ changes sign when $Q'^2 > Q^2$, which is the distinguishable signature of DDVCS process.

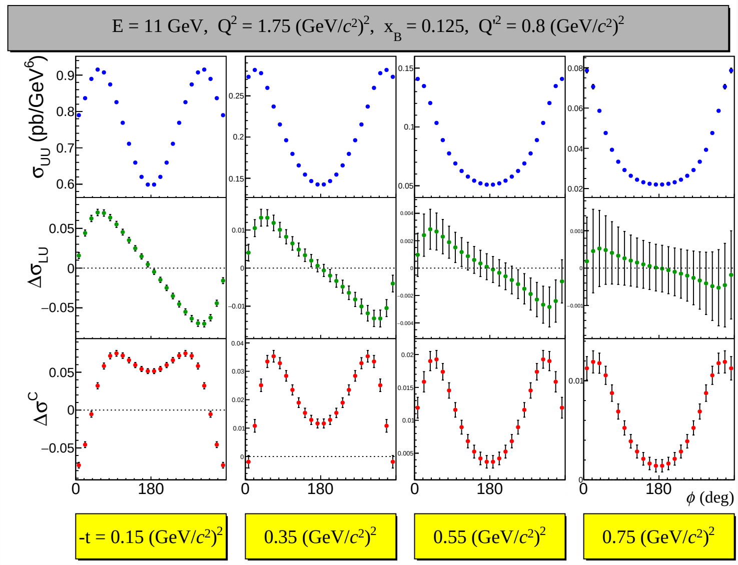

t-dependence: The cross sections and precisions decrease with increased $-t$.

CFFs phase space

$$\xi' = \frac{Q^2 - Q'^2 + t/2}{2Q^2/x_B - Q^2 - Q'^2 + t} \qquad \xi = \frac{Q^2 + Q'^2}{2Q^2/x_B - Q^2 - Q'^2 + t}$$

$$\mathcal{H}(\xi', \xi, t) = \sum_q e_q^2 \left\{ \mathcal{P} \int_{-1}^{1} dx\, H^q(x, \xi, t) \left[\frac{1}{x - \xi'} + \frac{1}{x + \xi'} \right] - i\pi \left[H^q(\xi', \xi, t) - H^q(-\xi', \xi, t) \right] \right\}$$

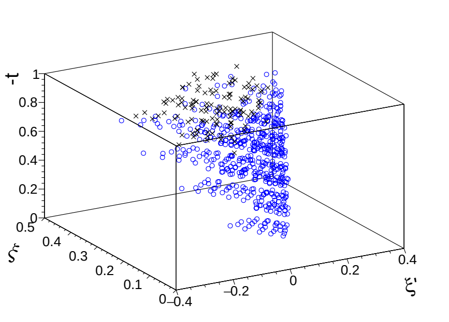

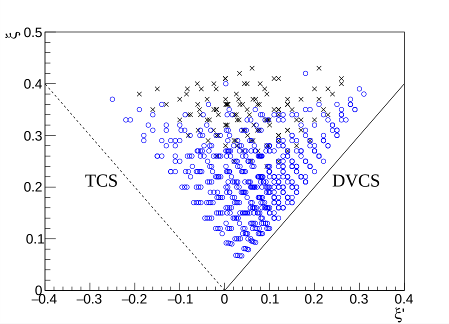

	no obs. $<10\%$	$\delta\sigma_{UU}/\sigma_{UU} < 10\%$
number of bins	120	544
ratio	18%	82%

CFFs phase space - real part

$$\mathcal{H}(\xi', \xi, t) = \sum_q e_q^2 \left\{ \boxed{\mathcal{P} \int_{-1}^{1} dx\, H^q(x, \xi, t) \left[\frac{1}{x - \xi'} + \frac{1}{x + \xi'} \right]} - i\pi \left[H^q(\xi', \xi, t) - H^q(-\xi', \xi, t) \right] \right\}$$

- σ_{UU} and $\Delta\sigma^{\mathrm{C}}$ are both sensitive to real part of CFFs;
- $\Delta\sigma^{\mathrm{C}}$ has better precision in fitting CFFs (only one contribution of σ_{INT1}).

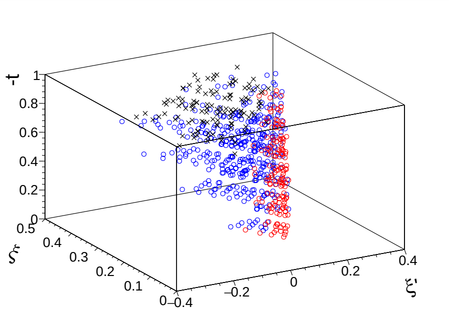

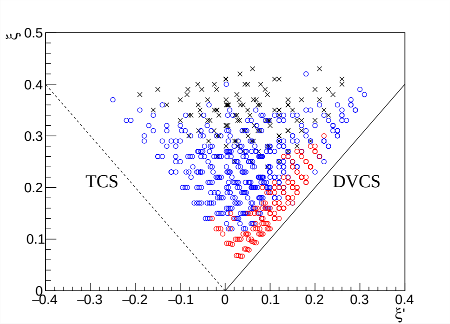

	no obs.$<10\%$	$\frac{\delta\sigma_{\mathrm{UU}}}{\sigma_{\mathrm{UU}}} < 10\%$ & $\frac{\delta\Delta\sigma^{\mathrm{C}}}{\Delta\sigma^{\mathrm{C}}} > 10\%$	$\frac{\delta\Delta\sigma^{\mathrm{C}}}{\Delta\sigma^{\mathrm{C}}} < 10\%$
number of bins	120	396	148
ratio	18%	60%	22%

CFFs phase space - imaginary part

$$\mathcal{H}(\xi',\xi,t) = \sum_q e_q^2 \Big\{ \mathcal{P}\int_{-1}^{1} dx\, H^q(x,\xi,t) \left[\frac{1}{x-\xi'} + \frac{1}{x+\xi'} \right] - i \boxed{\pi \left[H^q(\xi',\xi,t) - H^q(-\xi',\xi,t) \right]} \Big\}$$

- $\Delta\sigma_{\mathrm{LU}}$ is sensitive to imaginary part of CFFs being able to directly access to GPDs.

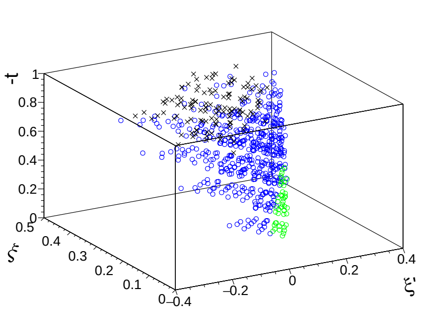

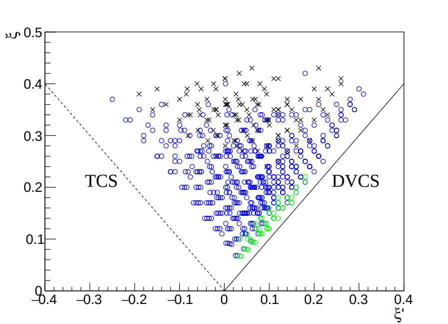

	no obs.<10%	$\frac{\delta\sigma_{\mathrm{UU}}}{\sigma_{\mathrm{UU}}}$ <10% & $\frac{\delta\Delta\sigma_{\mathrm{LU}}}{\Delta\sigma_{\mathrm{LU}}}$ >10%	$\frac{\delta\Delta\sigma_{\mathrm{LU}}}{\Delta\sigma_{\mathrm{LU}}}$ <10%
number of bins	120	498	46
ratio	18%	75%	7%

- increasing $\mathscr{L}$ to 10^{39} $\mathrm{cm}^{-2}\mathrm{s}^{-1}$ (100 times larger);

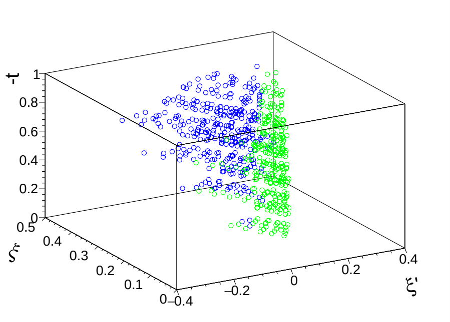

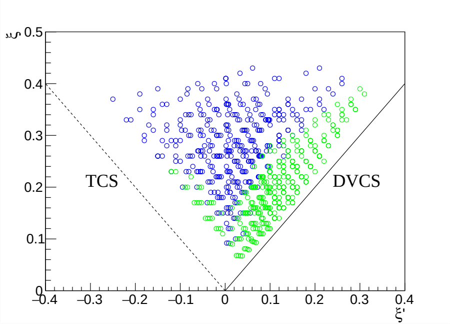

	no obs.<10%	$\frac{\delta\sigma_{UU}}{\sigma_{UU}}$ <10% & $\frac{\delta\Delta\sigma_{LU}}{\Delta\sigma_{LU}}$ >10%	$\frac{\delta\Delta\sigma_{LU}}{\Delta\sigma_{LU}}$ <10%
number of bins	0	344	320
ratio	0%	52%	48%

- modification of the bin size to increase the statistics.

Summary and outlook

Summary:

- At a challenging luminosity (10^{37} $\mathrm{cm}^{-2}\mathrm{s}^{-1}$), it is possible to obtain DDVCS experiment observables with good precision.
- At large $-t$ and Q'^2 the bin size should be modified due to the small cross section and insufficient statistics.
- The sign change behavior of $\Delta\sigma_{\mathrm{LU}}$ is predicted and we are looking forward to see this typical signature in a prospective experiment.

Outlook:

- Extraction of CFFs;
- DDVCS at EIC.
  - High energy expands the DDVCS phase space;
  - High energy leads to larger cross section and possibility for the study of the decay angles dependence of cross section (7-fold differential cross section);
  - Possibility of polarized proton ($\Delta\sigma_{\mathrm{UL}},\ \Delta\sigma_{\mathrm{LL}}$) and polarized positron ($\Delta\sigma^{\mathrm{C}}_{\mathrm{LU}}$).

Thank you!

back up

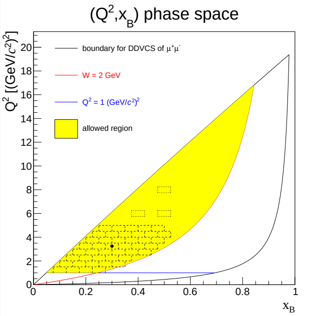

Test of the bins at $Q^2 > 5\ (\mathrm{GeV}/c^2)^2$

- very limited allow region for $-t$;
- smaller cross sections and worse precision.

Q^2 $(\mathrm{GeV}/c^2)^2$	x_B	$-t$ $(\mathrm{GeV}/c^2)^2$	Q'^2 $(\mathrm{GeV}/c^2)^2$	$\delta\sigma_{UU}/\sigma_{UU}$ (%)	$\delta\Delta\sigma_{LU}/\Delta\sigma_{LU}$ (%)	$\delta\Delta\sigma^C/\Delta\sigma^C$ (%)
6	0.4	0.5	0.3	3.82	21.7	28.3
			0.8	7.83	46.9	55.5
		1	0.3	6.29	48.8	21.4
			0.8	14.4	96.7	53.7
	0.5	0.5	0.3	7.04	84.8	188
		1	0.3	10.7	77.0	45.4
			0.8	22.7	173	112
8	0.5	0.8	0.3	7.98	59.5	107
			0.8	16.6	125	211
			1.3	24.8	251	448

back up

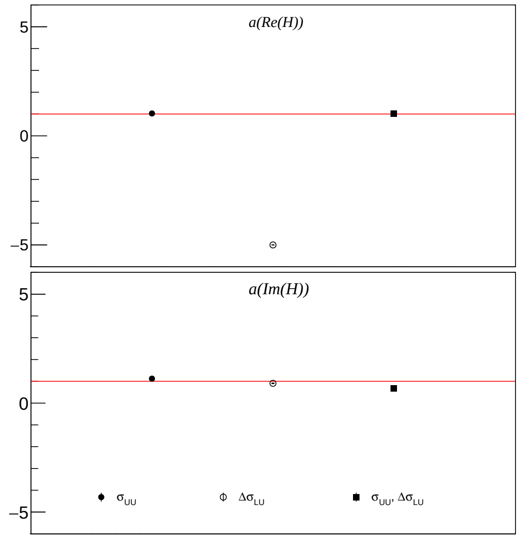

a(Re(H))
5
0
−5
a(Im(H))
5
0
−5
σ_{UU}
$\Delta\sigma_{LU}$
σ_{UU}, $\Delta\sigma_{LU}$